The Knee 21 (2014) 224–231

Contents lists available at ScienceDirect

The Knee

Finite element comparison of retrograde intramedullary nailing and locking plate fixation with/without an intramedullary allograft for distal femur fracture following total knee arthroplasty

Shih-Hao Chen [a], Ming-Chieh Chiang [b], Ching-Hua Hung [b,*], Shang-Chih Lin [c], Hsiao-Wei Chang [b]

[a] Department of Orthopedics, Tzu-Chi General Hospital at Taichung, and Tzu Chi University, Taiwan
[b] Department of Mechanical Engineering, National Chiao Tung University, Hsinchu, Taiwan
[c] Graduate Institute of Biomedical Engineering, National Taiwan University of Science and Technology, Taipei, Taiwan

ARTICLE INFO

Article history:
Received 17 September 2012
Received in revised form 3 March 2013
Accepted 6 March 2013

Keywords:
Distal femur fracture
Knee arthroplasty
Intramedullary
Retrograde nail
Intramedullary allograft
Osteoporotic femur

ABSTRACT

Purpose: Periprosthetic distal femur fracture after total knee arthroplasty due to the stress-shielding phenomenon is a challenging problem. Retrograde intramedullary nail (RIMN) or locking plate (LP) fixation with/without a strut allograft has been clinically used via less invasive stabilization surgery (LISS) for the treatment of these periprosthetic fractures. However, their biomechanical differences in construct stability and implant stress have not been extensively studied, especially for the osteoporotic femur.
Methods: This study used a finite-element method to evaluate the differences between RIMN, LP, and LP/allograft fixation in treating periprosthetic distal femur fractures. There were sixteen variations of two fracture angles (transverse and oblique), two loading conditions (compression and rotation), and four bony conditions (one normal and three osteoporotic). Construct stiffness, fracture micromotion, and implant stress were chosen as the comparison indices.
Results: The LP/allograft construct provides both lateral and middle supports to the displaced femur. Comparatively, the LP and RIMN constructs, respectively, transmit the loads through the lateral and middle paths, thus providing more unstable support to the construct and high stressing on the implants. The fracture pattern plays a minor role in the construct stabilization of the three implants. In general, the biomechanical performances of the RIMN and LP constructs were comparable and significantly inferior to those of the LP/allograft construct. The bone quality should be evaluated prior to the selection of internal fixators.
Conclusions: The LP/allograft construct significantly stabilizes the fracture gap, reduces the implant stress, and serves as the recommended fixation for periprosthetic distal femur fracture.

1. Introduction

Distal femur fractures adjacent to total knee arthroplasty (TKA) present a rare and yet complex problem, with an incidence ranging from 0.3% to 2.5% after primary surgery and from 1.6% to 3.8% after revision surgery [1,2]. The occurrence of periprosthetic supracondylar femur fractures can be attributed to the stress-shielding effects around the periprosthetic region [3–6]. Successful treatment requires regaining a painless, well aligned knee with a satisfactory range of motion and maintaining good alignment of the entire lower limb.

A wide variety of orthopedic devices had been used for the internal fixation of these fractures including angled blade plates, dynamic condylar plates, buttress plates, and flexible or rigid intramedullary nails [7]. Recently, periarticular locking plate (LP) or retrograde intramedullary nail (RIMN) fixation has become a popular treatment option with the less invasive stabilization system (LISS). The major advantage of LP is the ability to implant them with minimal soft tissue dissection, periosteal stripping, and multiple fixed-angle screws fixation around the fracture site to maintain distal fixation. Rigid RIMN can also be an effective device for minimally invasive stabilization of these fractures, and is considered if the patient has an open box femoral component for device access and adequate distal fracture fragments for locking fixation [8,9].

With unstable nail-bone contact, the construct stability of antegrade nailing for a periprosthetic fracture is weaker than that of the locking plate [10–12]. Comparatively, the retrograde nail makes deeper contact with the subchondral bone and operates in a minimally invasive fashion [13]. Consequently, RIMN has been recommended as an alternative for the treatment of periprosthetic fracture [14–17]. For LP fixation, the multiple points of cortical screws can provide better angular stability and secure bony anchoring for constructing stiffness and preservation of vascular supply [18–21]. However, the stress-shielding effect around the periprosthetic region potentially makes proximal screw loosening a major concern when using LISS plates [10–12,22,23]. Gardner et al. [24]

* Corresponding author at: National Chiao Tung University Mechanical Engineering, 1001 University Road, Hsinchu, 30010, Taiwan. Tel.: +886 3 571 2121 55160.
E-mail address: chhung@mail.nctu.edu.tw (C.-H. Hung).

0968-0160/$ – see front matter © 2013 Elsevier B.V. All rights reserved.
http://dx.doi.org/10.1016/j.knee.2013.03.006

used an intramedullary strut allograft to serve as the mechanical support supplemented to the LISS plate (LP/allograft) fixation, and declared that the hybrid use of LP/allograft can significantly stabilize the construct and facilitate the bony union. However, the complication rate is still 15–20% due to nonunion, malunion, infection, hardware failure or mortality even after RIMN or LP fixation for distal femur fractures following TKA [16,17,20,22,24]. However, biomechanical comparisons among RIMN, LP, and LP/allograft have not been extensively investigated.

Therefore, this study used the finite-element method to compare the construct behaviour subject to the variations of three internal fixations, two loading conditions, two fracture patterns, and four bony strengths. The convergence and stiffness of the intact model was validated. Then, the construct behaviour was evaluated in terms of construct stiffness, fracture micromotion, and implant stress. The purposes of this study provide biomechanical information about the differences among RIMN, LP, and LP/allograft, and point to which one should be indicated individually for various types of periprosthetic fractures following TKA. This study hypothesized that LP/allograft construct significantly stabilized fracture gap, reduced implant stress, and is potentially suitable for the treatment of periprosthetic distal femur fracture with comminution, deficient bone stock, and severe osteoporosis.

2. Methods

This study used the abbreviations LP and RIMN to denote the periarticular locking plate and retrograde intramedullary nail. The LP, RIMN, and LP/allograft fixations were compared in terms of two fracture patterns: transverse (TP, TN, and TA) and oblique (OP, ON, and OA). The femoral strengths were simulated by the three osteoporotic conditions: ost-1 (mild), ost-2 (moderate), ost-3 (severe).

2.1. Models of femur and implants

A femoral model was developed from the CT-scanned images of a mild-aged male (age: 45 years, weight: 60 kg, and height: 176 cm). The femur consists of cortical shell and cancellous core (Fig. 1a and b). Periprosthetic fracture was simulated as a displaced 1-cm gap that is the worst-case condition for transferring the femoral loads (Fig. 1c and d). This study used two patterns of the periprosthetic fractures (transverse and oblique) to evaluate the effects of the fracture pattern on the construct stability. Prior to instrumentation, the intact femur was validated by comparing the predicted stiffness with the experimental data of Koval's study [25]. This study used ANSYS version 12.0 (ANSYS Inc., USA) to perform construct stiffness analysis. The mesh size of the intact femur was determined by a convergence test of the construct stiffness *vs.* element number.

Three implants were instrumented into the fractured femur, including a knee prosthesis, RIMN, and LISS plate (Fig. 1). The knee prosthesis was a Zimmer Natural-Knee II PS (Zimmer Inc., Indiana, USA). The RIMN was 10 mm in diameter and 240 mm in length (TRIGEN, Smith and Nephew, USA). The LISS plate was 240 mm in length and 3 mm in thickness (AO Synthes, Pennsylvania, USA). The outer diameter, inner diameter, and length of the allografts were 17, 10, and 60 mm, respectively. All implants were instrumented into the femoral models according to standard surgical procedure.

A 9-hole LISS plate was fixed to the distal femur with five proximal and six distal cortical screws according to the manufacturer's instructions (Figs. 1 and 2). The RIMN was secured by two proximal and two distal interlocking screws. For the LISS plate with an allograft, the allograft was fixed using distal locking screws without penetrating the allograft surface. The allograft was secured against the medial cortex of the femur to ensure maximal medial support (Fig. 2c). In total, there were six variations of three implants and two fracture patterns (Fig. 2).

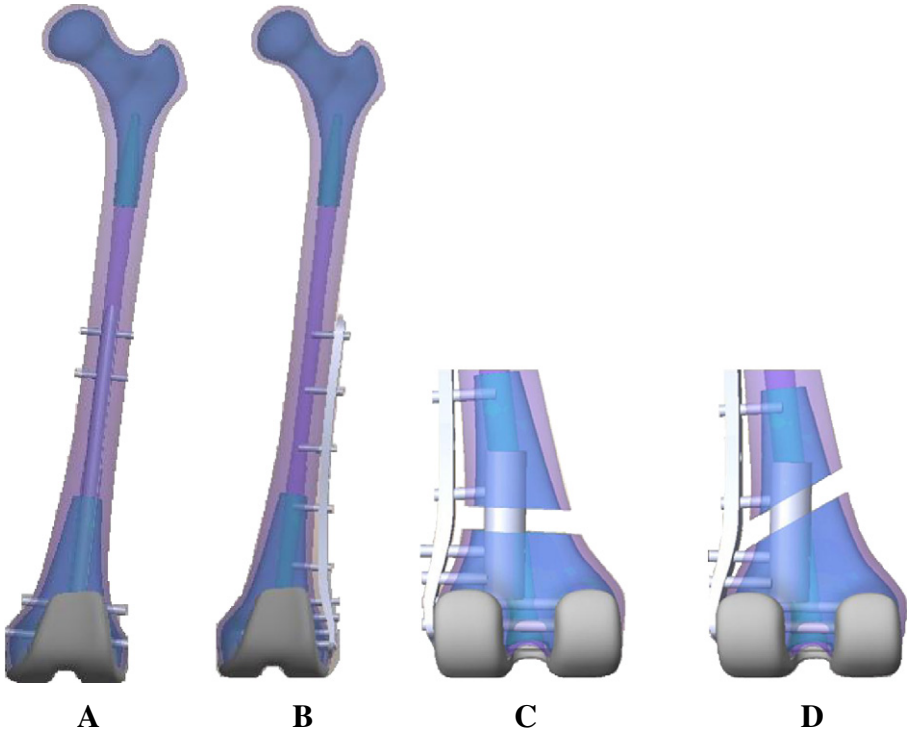

Fig. 1. Internal fixators and fracture patterns used in this study. (A) Retrograde nailing. (B) LISS plating. (C) Transverse fracture. (D) Oblique fracture.

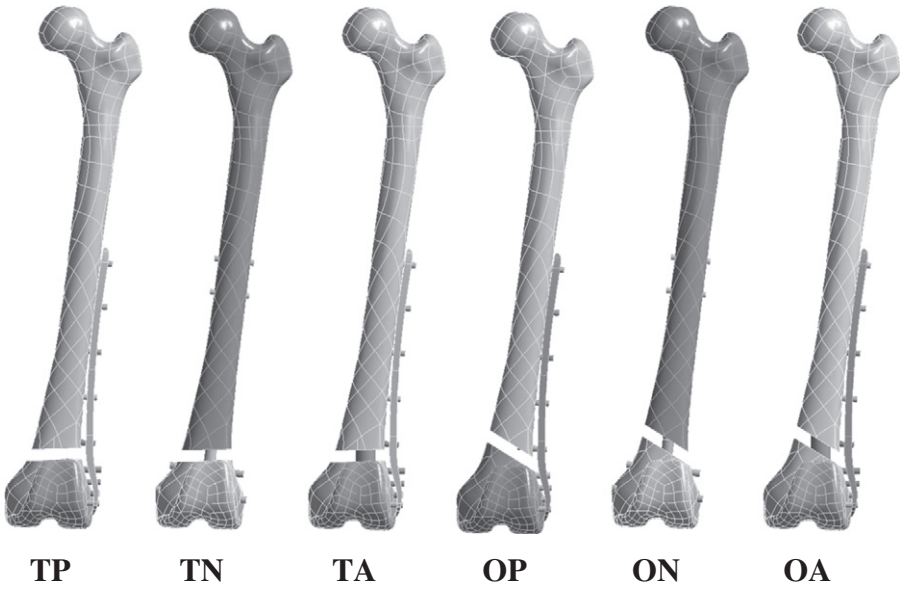

Fig. 2. Six variations of three internal fixations and two bone fractures. T: transverse fracture. O: oblique fracture. N: nail. P: plate. A: allograft.

2.2. Finite-element analysis

Four bone conditions were used to simulate osteoporosis around the supracondylar region. Normal cases denoted healthy bone above and below the fracture gap. The bone modulus of the ost-1 and ost-3 was decreased by 33% and 86% for cortical bone and 66% and 86% for cancellous bone, respectively [26–29]. For the ost-2 case, the decayed moduli of the cortical and cancellous bones were the same as those of the ost-1 and the degeneration of the distal bones was similar to that of the ost-3. In general, the ost-2 was the most common condition of the implant-induced osteoporosis at the periprosthetic region [26]. The material properties of the bones and implants were assumed to be isotropic and linearly elastic, as shown in Table 1. The calculated von Mises stresses of all implants were compared with the yielding strength of the corresponding material to validate the assumption of linear elasticity.

The threads of the cortical screws and plate holes were omitted to simplify finite-element analysis. The contact behavior of the screw/bone and screw/plate interfaces was set as fully bonded to ensure the load transmission from the femur to the implant. However, friction coefficients of the nail/bone, allograft/bone, and screw/allograft were 0.08, 0.3, and 0.8, respectively [30,31]. Two types of knee loads, compression and rotation were applied at the knee condyles (Fig. 3). The compression simulated a one-leg standing condition of a subject weighing about 50-kg. 60% of the 500-N compression was distributed to the medial condyle and the remaining was exerted on the lateral condyle (Fig. 3a) [32]. During walking, the screw-home mechanism induces the rotation moment at the knee joint (Fig. 3b). For rotation, a 6-Nm torque was applied to the distal femur and the surface nodes of the proximal femur were fully constrained [33]. The construct stability was monitored in terms of axial and rotational micromotion at the fracture gap. The axial micromotion was defined as the height change in the points *aa* (lateral), *bb* (middle), and *cc* (medial) (Fig. 3c). The rotation of the proximal and distal femora was measured as the rotational micromotion. The changes in the inclined angles between the lines *dd* and *ee* were projected along the same line onto the lower and upper surfaces of the fracture gap (Fig. 3c).

Table 1
Material properties of bones and implants.

Material	Elastic Modulus (MPa)	Poisson's Ratio (dimensionless)	Yield Strength (MPa)	References
Bones				
normal				
Cortical Shell	12,400	0.30	–	
Cancellous Core	104	0.30	–	
ost-1				[29]
Cortical Shell	8308	0.30	–	
Cancellous Core	35.36	0.30	–	
ost-2 upper part				[29]
Cortical Shell	8308	0.30	–	
Cancellous Core	35.36	0.30	–	
ost-2 lower part				[3,26–28]
Cortical Shell	2,027	0.30	–	
Cancellous Core	17	0.30	–	
ost-3				[26–28]
Cortical Shell	2,027	0.30	–	
Cancellous Core	17	0.30	–	
Implants				
fixators	110,000	0.30	800	
knee prostheses	210,000	0.30	–	
allograft	12400	0.30	–	

3. Results

3.1. Model validation

Fig. 4 showed the validation of the current study in terms of result convergence and construct stiffness. The construct stiffness was defined as the ratio of the vertical displacement at the medial points *cc* to the applied loads (Fig. 3c). During validation of construct stiffness, the intact femur was subject to the same loads as in Koval's study [25] and the experiment test. The construct stiffness converged to 1,226 N/mm until the element number reached about 72,000. The element size was set as 3 mm in this study, except at the bone/implant interfaces (Fig. 4a). For the convergent stiffness, the error of our study and Koval's study was only 0.3% (Fig. 4b). This indicates that good agreement was achieved and the intact femur was validated for further analyses.

3.2. Construct stiffness

Comparisons between the axial stiffness of the different constructs are shown in Fig. 5a. Except for the ost-3 bone, the TA construct significantly provided the highest stiffness. The stiffness values of the TP and TN constructs were comparable under all bone conditions. For the normal bone, the stiffness of the TA construct was about 95% higher than those of the TP and TN constructs. For the ost-1 bones, the stiffness difference between the TA construct and the other counterparts was reduced to 45% on average. For the ost-2 bones, the stiffness of the TA construct was 57% and 29% higher than those of the TP and TN constructs. For the ost-3 bone, the TA and TN

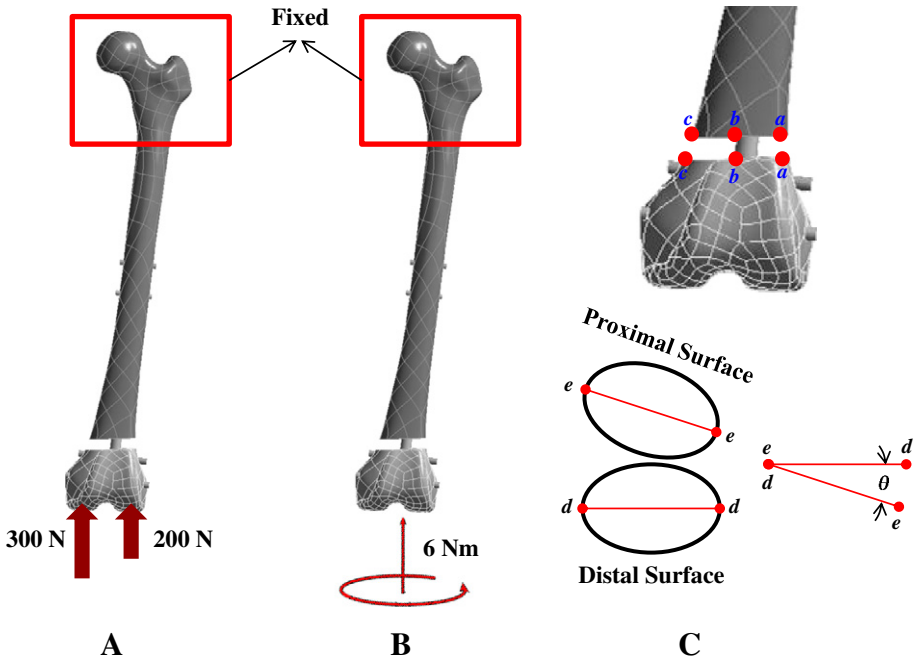

Fig. 3. Boundary and loading conditions of the femoral models. (A) Compression. (B) Rotation. (C) Five lines from *aa* to *ee* were used to calculate the axial and rotational micromotion of the fracture gap.

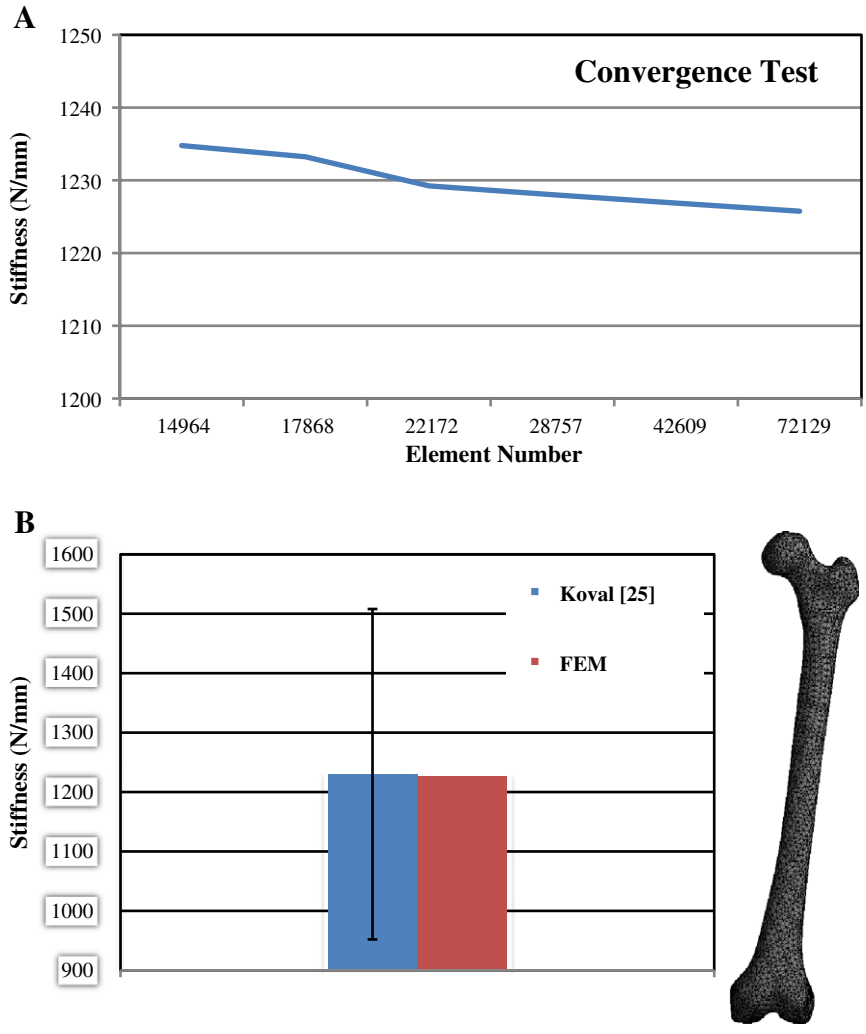

Fig. 4. (A) Convergence test of the intact model. (B) Stiffness comparison between this study and previous studies.

constructs exhibited comparable stiffness and were slightly stiffer than the TP construct. On average, the stiffness of the ost-1 construct was 12%, 139% higher than that of the ost-2 and ost-3 constructs, respectively. The results of the oblique and transverse fractures were similar.

Fig. 5b shows the results of rotational stiffness for the different constructs. Similar to axial stiffness, fracture pattern plays a minor role in rotational stiffness. Under all bone conditions, the TA construct was the stiffest, followed by the TP construct, and the TN construct was the weakest. However, the rotational stiffness of the ost-3 condition was comparable among all three implants. For all implants, the construct stiffness of the ost-1 condition was the highest and the ost-3 condition was the least. On average, the construct stiffness of the ost-1 condition was 8% higher than that of ost-2. However, the stiffness difference between the ost-1 and ost-3 conditions increased to 93%.

3.3. Fracture micromotion

The axial and rotational stability was evaluated by the fracture micromotion, as shown in Fig. 6. The results of the axial and rotational micromotions were similar for the transverse and oblique fractures. For the axial loading, the lateral gap of the TN construct was the most unstable and the micromotion of the TA construct was the least unstable (Fig. 6a). For the middle micromotion, the TP construct provided the weakest support to the medial fracture and the micromotion of the TA construct was the highest, except for the ost-3 bone (Fig. 6b). Under normal and ost-2 conditions, the micromotion of the TP construct was respectively 80% and 152% higher than those of the TN and TA constructs. For the medial micromotion, the TA construct provided the highest fracture-stabilizing ability in comparison to the other counterparts (Fig. 6c). Under the normal and ost-2 conditions, the micromotion of the TA construct was respectively 58% and 44% less than those of the TN and TA constructs. For the rotational loading, the micromotion of the TN construct was comparable for all bone conditions and consistently higher than those of the TP and TA constructs (Fig. 6d). For the normal and ost-2 bones, the rotational micromotion of the TN construct was respectively 1.91 and 2.83 times those of the TP and TA constructs.

3.4. Implant stress

Fig. 7 shows the comparison of maximum von Mises stress among the implants instrumented into the ost-2 bone. For axial and rotational loading, the sequence of the implant stresses was similar among transverse and oblique fractures. For the axial loading, the stress value of the TP construct was respectively 22% and 132% higher than those of the TN and TA constructs (Fig. 7a). The maximum stresses of all implants consistently occurred around the fracture sites. For the rotational loading, the stress of the TN construct was 27% and 90% higher than those of the TP and TA construct, respectively. The TP and TA implants were highly stressed at the plate holes proximal to the fracture gap. The highest stress of the TN construct occurred at the second proximal screw (Fig. 7a).

4. Discussion

From the biomechanical viewpoint, the RIMN, LP, and LP/allograft were the representatives of the middle, lateral, and middle/lateral support to the femur, respectively (Fig. 1). Fig. 8 schematically shows the load-transferring paths from the knee condyles to the proximal femur: through plate (line *pp*), nail (line *nn*), and allograft (line *gg*). The implant-induced support to the displaced femur was evaluated in terms of construct stiffness, fracture micromotion, and implant stress in this study. Without bony union, this study aimed

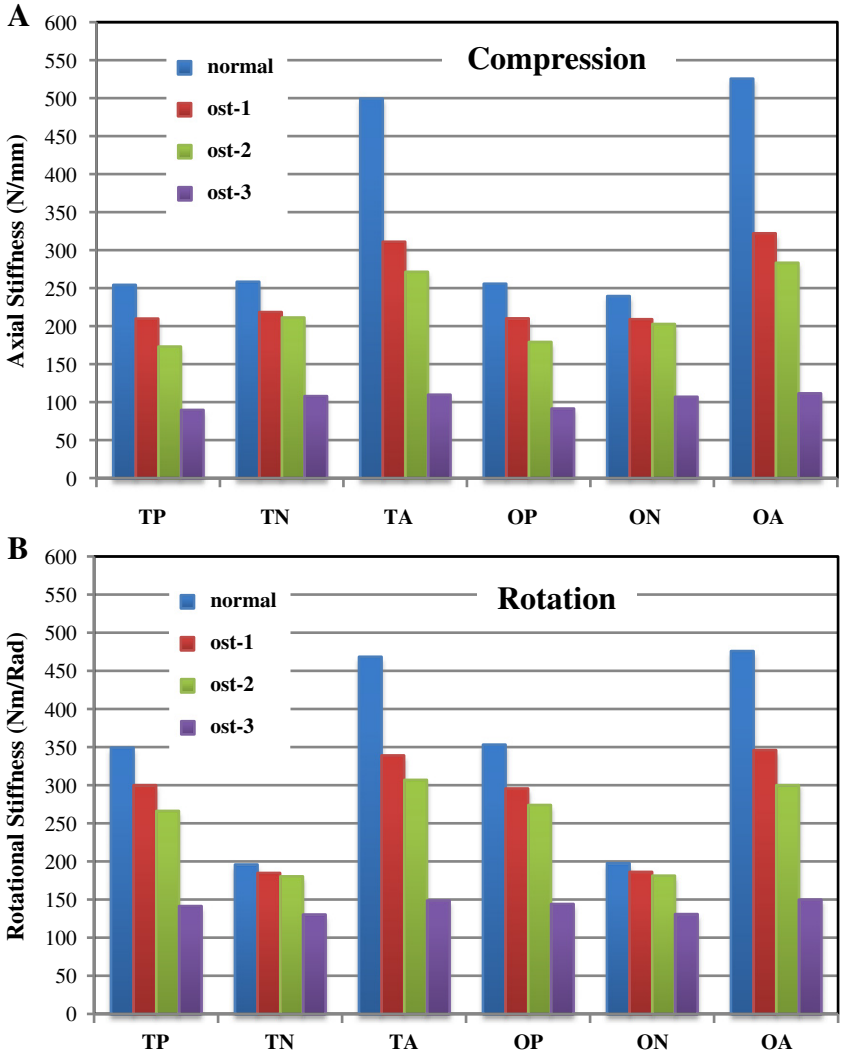

Fig. 5. Comparison of the construct stiffness of all models under (A) Compression. (B) Rotation.

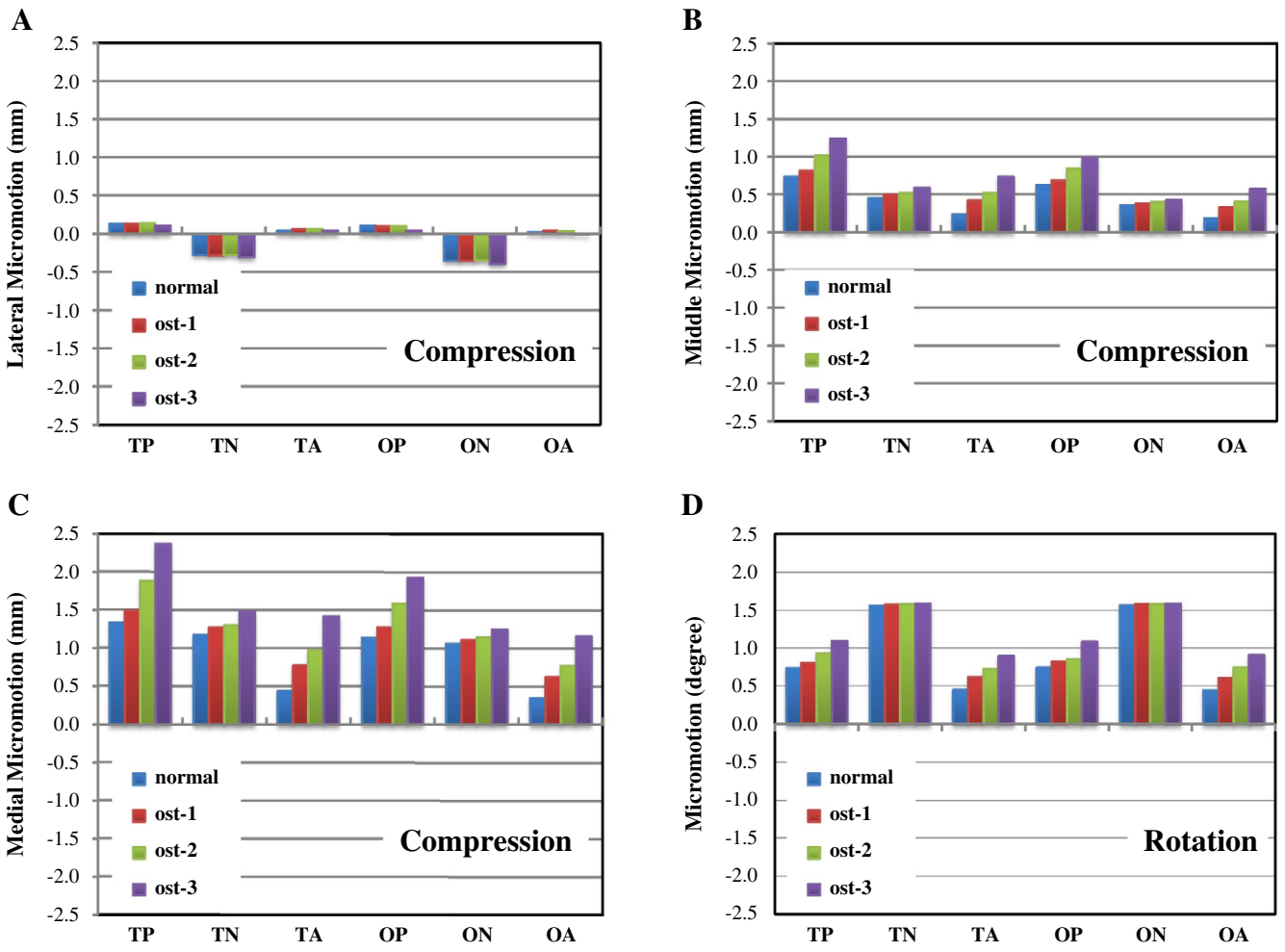

Fig. 6. Comparison of the construct micromotion of all models under (A-C) Lateral, middle, and medial micromotion of compression (D) Rotational micromotion.

to compare the construct stability of the three implants within the immediate postoperative period.

For construct stability, the LP/allograft construct exhibited the highest stiffness and the least micromotion (Figs. 5 and 6). This can be attributed to the reason that the knee loads of the LP/allograft construct are transferred through the paths of lines *pp* and *gg* (Fig. 8a and c). Although Schutz's and *Ricci's* studies claim that only the LISS plate can provide stable fixation for the periprosthetic supracondylar femur fractures [19,34], this study demonstrated that the allograft can partially transmit the knee loads to the proximal femur and decrease the moment arm between the allograft and condyles (Fig. 8c). This reduced the mechanical demands of the lateral LISS and made the LP/allograft more stable and less stressed. For the axial stiffness, the lateral plate and middle nail provided comparable stiffness (Fig. 5a). For the RIMN construct, the RIMN was approximately in the position of the femoral axis and was inefficiently resistant to the rotational loads. This can explain why the rotational stiffness and micromotion of the RIMN construct were the least and most unstable among the counterparts. On the middle and medial sides, the fracture-stabilizing ability of the LISS construct was the least due to the longer moment arm of the lateral fixation (Fig. 6b and c). The moment arm between the middle allograft and the lateral plate can constitute a rotation-resisting mechanism to stabilize the twisted femur (Fig. 8c). Compared with the LP/allograft construct, the LISS plate and screws must have been highly stressed, making them potential sites for plastic yielding and fatigue cracking (Fig. 7) [35,36].

After surgery, this study revealed that the fracture patterns have little effect on the construct stiffness, fracture micromotion, and implant stress from the axial and rotational loadings (Figs. 5–7). This can be explained by the fact that the fracture fragments were displaced by 1-cm gap and the load-transferring function of the facture gap was assumed to be totally disabled (Fig. 1). Under such circumstances, the biomechanical behaviors of the femoral construct were determined by the implant properties. This study further showed that the axial stiffness and medial micromotion of the RIMN and LP constructs were comparable (Figs. 5a and 6c). This finding was similar to the result of the Bong's and Hou's studies [32,37] where the RIMN and LP provided similar fixation of fractures without significant comminution. However, the rotational stiffness and micromotion were still significantly different, except for with the osteoporotic bones (Figs. 5b and 6a-d). This can be explained by the fact that the RIMN provides inefficient rotation-resisting ability to the displaced femur. In Heiney's study [38], the RIMN also showed superior ability to stabilize the facture over the locking compression plate under different magnitudes of axial loading.

This study focused on the biomechanical comparison between the three internal fixations. Consequently, the micromotion and

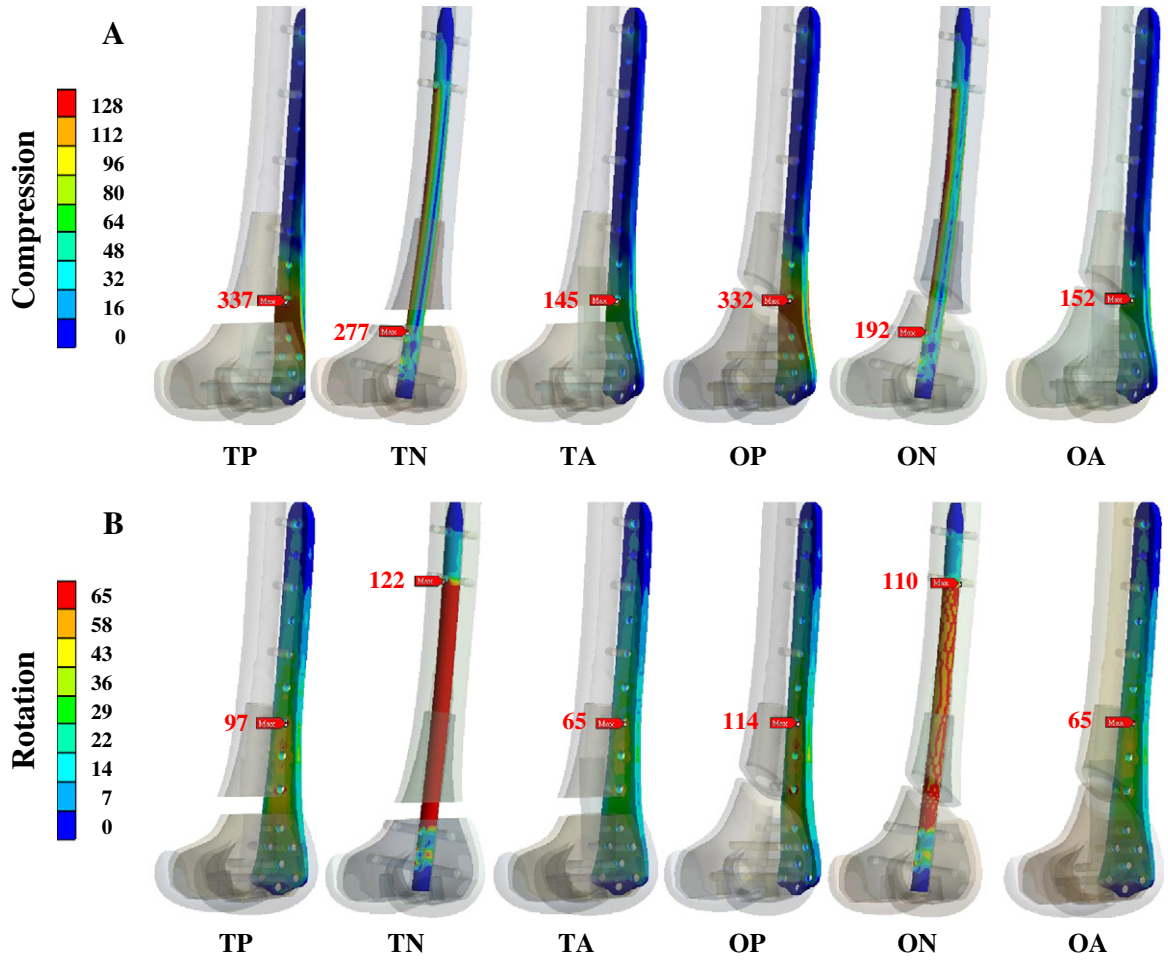

Fig. 7. Comparison of the maximum implant stress under (A) Compression (B) Rotation.

loosening at the screw/plate and screw/bone interfaces were not simulated due to the convergence problem of the highly nonlinear analysis. If the back-out of the screws from the plate and bone occurs, the instability of the entire construct might reduce the biomechanical difference between the three fixations. However, this should be further investigated by experimental rather than numerical methods due to the fact of interfacial nonlinearity.

For the ost-3 bone, the axial and rotational stiffness of the TP, TN, and TA construct were comparable (Fig. 5). However, the stiffness differences between the TA and TN constructs were about 93% (axial) and 139% (rotational) for the normal bone. For micromotion, bone quality had a minor effect on the RIMN in comparison to other constructs (Fig. 6). This was attributed to the two fixation mechanisms: screws and plate. For the screw fixation, the LP screws were fully inserted into the cancellous bone and only two ends of the RIMN screws were fixed at the cortical bone. This makes the mechanical support of the LP screws more sensitive to the decay of the bone quality when compared with the nail screws. Lin *et al.* showed that the nail-cancellous contact plays a minor role in maintaining the construct stability with the supracondylar region [39]. Consequently, the deflection of the lateral plate relies more on the structural properties of the distal femur than on the nail. This indicates that quality verification of the periprosthetic bone is essential prior to internal fixation [28].

In conclusion, bone quality is one of the key factors when treating periprosthetic supracondylar factures. Compared with the LP/allograft construct, the LP and RIMN constructs provided more comparable performance. However, the mechanical failure of highly stressed LP and RIMN is one the major concerns for osteoporotic and overweight patients. The use of the LP/allograft significantly stabilizes the fracture gap and reduces the implant stress, making it potentially suitable for the treatment of periprosthetic distal femur fractures.

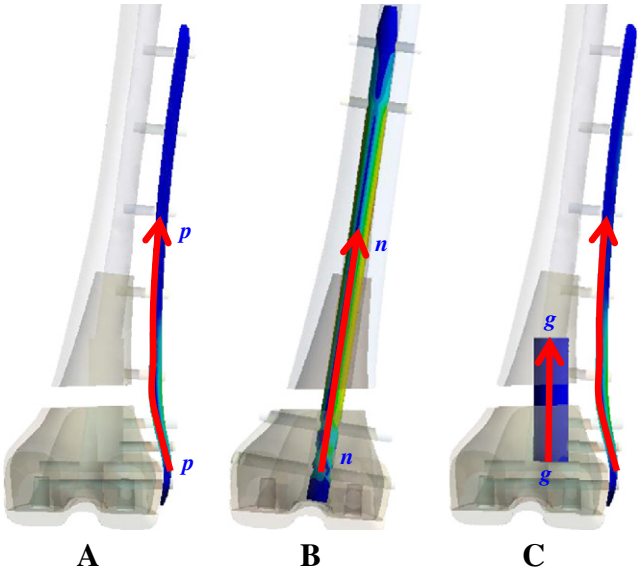

Fig. 8. Schematical diagrams showing load-transferring paths from the distal to proximal femurs. (A) The LP contact, line *pp*. (B) The nailing construct, line *nn*. (C) The LP/allograft construct, line *gg*.

5. Conflict of interest statement

The authors report no conflict of interest in this project.

References

[1] Cain PR, Rubash HE, Wissinger HA, McClain EJ. Periprosthetic femoral fractures following total knee arthroplasty. Clin Orthop Relat Res 1989;208:205–14.
[2] DiGioia AM, Rubash HE. Periprosthetic fractures of the femur after total knee arthroplasty: a literature review and treatment algorithm. Clin Orthop Relat Res 1991;271:135–42.
[3] Saari T, Uvehammer J, Carlsson LV, Regnér L, Kärrholm J. Posterior stabilized component increased femoral bone loss after total knee replacement. 5-year follow-up of 47 knees using dual energy X-ray absorptiometry. Knee 2006;13(6):435–9.
[4] Delpott PH, Van Audekercke R, Martens M. Conservative treatment of ipsilateral supracondylar femoral fracture after total knee arthroplasty. J Trauma 1984;24(9):846–9.
[5] Sochart DH, Hardinge K. Nonsurgical management of supracondylar fracture above total knee arthroplasty. Still the nineties option. J Arthroplasty 1997;12(7):830–4.
[6] Short WH, Hootnick DR, Murry DG. Ipsilateral supracondylar femur fractures following knee arthroplasty. Clin Orthop Relat Res 1981;158:111–6.
[7] Althausen PL, Lee MA, Finkemeier CG, Meehan JP, Rodrigo JJ. Operative stabilization of supracondylar femur fractures above total knee arthroplasty: a comparison of four treatment methods. J Arthroplasty 2003;18(7):834–9.
[8] Heiney JP, Battula S, O'Connor JA, Ebraheim N, Schoenfeld AJ, Vrabec G. Distal femoral fixation: a biomechanical comparison of retrograde nail, retrograde intramedullary nail, and prototype locking retrograde nail. Clin Biomech 2012;27(7):692–6.
[9] Leggon RE, Feldmann DD. Retrograde femoral nailing: a focus on the knee. Am J Knee Surg 2001;14(2):109–18.
[10] Moore TJ, Watson T, St. Green, Garland DE, Chandler RW. Complications of surgically treated supracondylar fractures of the femur. J Trauma 1987;27(4):402–6.
[11] Schatzker J. Fractures of the distal femur revisited. Clin Orthop Relat Res 1998;347:43–56.
[12] Wu CC, Shih CH. Distal femoral nonunion treated with interlocking nailing. J Trauma 1991;31(12):1659–62.
[13] Maier M, Marzi I. Elastic stable intramedullary nailing of femur fractures in children. Oper Orthop Traumatol 2008;20(4–5):364–72.
[14] Leung KS, Shen WY, So WS, Mui LT, Grosse A. Interlocking intramedullary nailing for supracondylar and intercondylar fractures of the distal part of the femur. J Bone Joint Surg Am 1991;73(3):332–40.
[15] Ostrum RF, Geel C. Indirect reduction and internal fixation of supracondylar femur fractures without bone graft. J Orthop Trauma 1995;9(4):278–84.
[16] Bolhofner BR, Carmen B, Clifford P. The results of open reduction and internal fixation of distal femur fractures using biologic (indirect) reduction technique. J Orthop Trauma 1996;10(6):372–7.
[17] Brumback RJ, Uwagie-Ero S, Lakatos RP, Poka A, Bathon GH, Burgess AR. Intramedullary nailing of femoral shaft fractures – Part II: Fracture-healing with static interlocking fixation. J Bone Joint Surg Am 1988;70(10):1453–62.
[18] Kolb W, Guhlmann H, Windisch C, Marx F, Koller H, Kolb K. Fixation of periprosthetic femur fractures above total knee arthroplasty with the less invasive stabilization system: a midterm follow-up study. J Trauma 2010;69(3):670–6.
[19] Schütz M, Müller M, Krettek C, Höntzsch D, Regazzoni P, Ganz R, et al. Minimally invasive fracture stabilization of distal femoral fractures with the LISS: a prospective multicenter study. Results of a clinical study with special emphasis on difficult cases. Injury 2001;32(3):48–54.
[20] Farouk O, Krettek C, Miclau T, Schandelmaier P, Guy P, Tscherne H. Minimally invasive plate osteosynthesis: does percutaneous plating disrupt femoral blood supply less than the traditional technique? J Orthop Trauma 1999;13(6):401–6.
[21] Tharani R, Nakasone C, Vince KG. Periprosthetic fractures after total knee arthroplasty. J Arthroplasty 2005;20(4):27–32.
[22] Gardner MJ, Weil Y, Barker JU, Kelly BT, Helfet DL, Lorich DG. The importance of medial support in locked plating of proximal humerus fractures. J Orthop Trauma 2007;21(3):185–91.
[23] Butt MS, Krikler SJ, Ali MS. Displaced fractures of the distal femur in elderly patients. J Bone Joint Surg Br 1996;78(1):110–4.
[24] Gardner MJ, Boraiah S, Helfet DL, Lorich DG. Indirect medial reduction and strut support of proximal humerus fractures using an endosteal implant. J Orthop Trauma 2008;22(3):195–200.
[25] Koval KJ, Kummer FJ, Bharam S, Chen D, Halder S. Distal femoral fixation: a laboratory comparison of the 95 degrees plate, antegrade and retrograde inserted reamed intramedullary nails. J Orthop Trauma 1996;10(6):378–82.
[26] Carter DR, Hayes WC. The compressive behavior of bone as a two-phase porous structure. J Bone Joint Surg Am 1977;59(7):954–62.
[27] Rho JY, Zerwekh JE, Ashman RB. Examination of several techniques for predicting trabecular elastic modulus and ultimate strength in the human lumbar spine. Clin Biomech 1994;9(2):67–71.
[28] Clark DI, Crofts CE, Saleh M. Femoral neck fracture fixation: comparison of a sliding screw with lag screws. J Bone Joint Surg Br 1990;72(5):797–800.
[29] Turner AW, Gillies RM, Sekel R, Morris P, Bruce W, Walsh WR. Computational bone remodelling simulations and comparisons with DEXA results. J Orthop Res 2005;23(4):705–12.
[30] Grant JA, Bishop NE, Gotzen N, Sprecher C, Honl M, Morlock MM. Artificial composite bone as a model of human trabecular bone: the implant–bone interface. J Biomech 2007;40(5):1158–64.
[31] Chen WP, Tai CL, Shih CH, Hsieh PH, Leou MC, Lee MS. Selection of fixation devices in proximal femur rotational osteotomy: clinical complications and finite element analysis. Clin Biomech 2004;19(3):255–62.
[32] Bong MR, Egol KA, Koval KJ, Kummer FJ, Su ET, Iesaka K, et al. Comparison of the LISS and a retrograde-inserted supracondylar intramedullary nail for fixation of a periprosthetic distal femur fracture proximal to a total knee arthroplasty. J Arthroplasty 2002;17(7):876–81.
[33] DesJardins JD, Walker PS, Haider H, Perry J. The use of a force-controlled dynamic knee simulator to quantify the mechanical performance of total knee replacement designs during functional activity. J Biomech 2000;33(10):1231–42.
[34] Ricci WM, Loftus T, Cox C, Borrelli J. Locked plates combined with minimally invasive insertion technique for the treatment of periprosthetic supracondylar femur fractures above a total knee arthroplasty. J Orthop Trauma 2006;20(3):190–6.
[35] Kumar A, Chambers I, Maistrelli G, Wong P. Management of periprosthetic fracture above total knee arthroplasty using intramedullary fibular allograft and plate fixation. J Arthroplasty 2008;23(4):554–8.
[36] Wilson D, Frei H, Masri BA, Oxland TR, Duncan CP. A biomechanical study comparing cortical onlay allograft struts and plates in the treatment of periprosthetic femoral fractures. Clin Biomech 2005;20(1):70–6.
[37] Hou Z, Bowen TR, Irgit K, Strohecker K, Matzko ME, Widmaier J, et al. Locked plating of periprosthetic femur fractures above total knee arthroplasty. J Orthop Trauma 2012;26(7):427–32.
[38] Heiney JP, Barnett MD, Vrabec GA, Schoenfeld AJ, Baji A, Njus GO. Distal femora fixation: a biomechanical comparison of trigen retrograde intramedullary (I.M.) nail, dynamic condylar screw (DCS), and locking compression plate (LCP) condylar plate. J Trauma 2009;66(2):443–9.
[39] Lin J, Lin SJ, Chen PQ, Yang SH. Stress analysis of the distal locking screws for femoral interlocking nailing. J Orthop Res 2001;19(1):57–63.